minerals

MDPI

Article

Selective Separation of La(III) and Ce(III) Using Hollow Fiber Membranes: Influence of pH and Extractant Systems

Felipe Olea [1,*], Laura Ulloa [2], Eugenio Bringas [2], Julio Urzúa-Ahumada [1], Ricardo Abejón [3], Julio Romero [3] and Esteban Quijada-Maldonado [1,*]

[1] Laboratory of Separation Processes Intensification (SPI), Department of Chemical and Bioprocess, University of Santiago de Chile, Av. Lib. Bdo. O'Higgins Engineering 3363, Estación Central, Santiago 9170020, Chile; julio.urzua@usach.cl

[2] Departmento de Ingenierías Química y Biomolecular, ETSIIyT, Universidad de Cantabria, Avda. Los Castros s/n, 39005 Santander, Spain; laurauloaguntinas@gmail.com (L.U.); eugenio.bringas@unican.es (E.B.)

[3] Laboratory of Membrane Separation Processes (LabProSeM), Department of Chemical and Bioprocess, University of Santiago de Chile, Av. Lib. Bdo. O'Higgins Engineering 3363, Estación Central, Santiago 9170020, Chile; ricardo.abejon@usach.cl (R.A.); julio.romero@usach.cl (J.R.)

* Correspondence: felipe.oleac@usach.cl (F.O.); esteban.quijada@usach.cl (E.Q.-M.)

Abstract: The selective separation of adjacent rare earth elements (REEs), such as La(III) and Ce(III), is a critical challenge in hydrometallurgy due to their similar chemical properties. This work evaluates the performance of non-dispersive solvent extraction (NDSX) using hollow fiber (HF) membranes for this purpose. Initial solvent extraction (SX) equilibrium experiments with Cyanex® 272 in kerosene determined that the aqueous phase's optimal pH for selectivity is 5.6, achieving a selectivity of $\alpha_{Ce/La}$ =12.7. NDSX experiments demonstrated enhanced selectivity $\alpha_{Ce/La} = 34$ after 120 min, benefiting from the additional mass transfer resistance provided by the HF membrane. Maintaining a constant pH of 5.0 with NaOH improved extraction rates but slightly reduced selectivity to $\alpha_{Ce/La} = 26$. Experiments using 1,1,1-trifluoro-2,4-pentanedione (HTFAC) in the ionic liquid (IL) [Omim][Tf2n] as the receiving phase showed lower extraction rates but achieved comparable selectivity values ($\alpha_{Ce/La} = 22$) in just 20 min, thanks to the IL's viscosity limiting La(III) extraction. The impact of HF membrane design was also assessed; increasing the membrane's surface area significantly improved extraction rates but reduced selectivity due to reduced mass transfer resistance. These results demonstrate the potential of NDSX systems for selective REE separation, particularly by leveraging controlled mass transfer and operating conditions. However, further work is needed to optimize system design. The findings highlight the advantages of NDSX over traditional SX, offering a promising pathway for sustainable and efficient REE processing.

Keywords: non-dispersive solvent extraction (NDSX); hollow fiber membranes; rare earth elements (REEs); ionic liquids (ILs)

Academic Editor: Sehliselo Ndlovu

Received: 19 December 2024
Revised: 23 January 2025
Accepted: 5 February 2025
Published: 11 February 2025

Citation: Olea, F.; Ulloa, L.; Bringas, E.; Urzúa-Ahumada, J.; Abejón, R.; Romero, J.; Quijada-Maldonado, E. Selective Separation of La(III) and Ce(III) Using Hollow Fiber Membranes: Influence of pH and Extractant Systems. *Minerals* **2025**, *15*, 167. https://doi.org/10.3390/min15020167

1. Introduction

Rare earth elements (REEs) comprise a group of 17 elements in the periodic table: the 15 lanthanides, spanning from lanthanum (La) to lutetium (Lu), as well as scandium (Sc) and yttrium (Y). The US Geological Survey (USGS) Mineral Product Summary 2020 data have reported that, as of the end of 2019, the world's rare earth resource reserves were 120 million tons. China's reserves had 37% of the world's reserves (44 million tons), becoming the country with the largest REE resources in the world, followed by Brazil

and Vietnam, which share the second place (22 million tons each). This is followed by Russia (12 million tons), India (6.9 million tons), Australia (3.3 million tons), Greenland (1.5 million tons), the United States (1.4 million tons), Canada (830,000 tons), South Africa (790,000 tons), and Tanzania (890,000 tons) [1].

Among the lanthanides, Ce and La are the most abundant REEs, which are typically found in minerals such as bastnasite and monazite [2]. These elements are essential for the advancement of modern industry due to their wide range of technological applications [3], such as high-efficiency magnets [4], batteries [5], compact electronic devices [6], capacitors [7], laser technologies [8], as well as telecommunications and high-precision instruments [9]. Cerium plays a critical role in various industrial processes owing to its unique catalytic properties [10–12]. Lanthanum, on the other hand, is widely used as a catalyst [13–16] and in the production of high-quality optical glass and lenses [17,18], among other applications.

The separation of cerium (Ce) and lanthanum (La) presents significant challenges due to their chemically similar properties, which complicates their effective fractionation and purification. Both elements exhibit nearly identical ionic radius and chemical behavior, making their separation particularly difficult. The traditional isolation process for these elements relies on solvent extraction (SX) [19–21], and the respective results are informed by the selectivity factor ($\alpha_{Ce/La}$), which indicates the ratio of extracted concentrations of Ce(III) from La(III), showing the separation efficiency. However, achieving high selectivity for the purification of specific lanthanides remains a challenge, especially when separating adjacent lanthanides. This results in the need for multiple equilibrium stages to achieve effective separation. For instance, Dzulqornain et al. [22] employed SX with commercially available extractants dissolved in kerosene to separate neodymium (Nd(III)) and praseodymium (Pr(III)), obtaining a maximum selectivity of $\alpha_{Nd/Pr}$= 1.6. Similarly, Belfqueh et al. [23] used N,N,N′,N′-tetraoctyldiglycolamide (TODGA) in aliphatic diluents, achieving a relatively low selectivity of $\alpha_{Nd/Pr} \approx 1.5$. Zhang et al. [24] applied a mixture of extractants in sulfonated kerosene, yielding a comparable $\alpha_{Nd/Pr}$= 1.4 and slightly higher values for Ce(III)/La(III) separation ($\alpha_{Ce/La}$ = 3.5). Tunsu et al. obtained a selectivity of 2.88 Ce/La when using Cyanex 923 and kerosene from nitric acid media [25]. Sharma et al. obtained a selectivity of 1.41 Ce/La when using a calix arene extractant in n-octanol [26].

Recently, ionic liquids (ILs) have been proposed as sustainable alternatives to organic solvents for the green purification of REEs [27,28] because ILs offer reduced volatility and are nonflammable, with lower toxicity and enhanced recyclability [29,30], making them an attractive option for green chemistry applications. In addition, the long-term sustainability of ILs lies in their potential to minimize hazardous waste in the environment. The stability and high extraction capacity of ILs reduce the amount of diluent required. Quinn et al. [31] employed bifunctional ILs for lanthanide fractionation, achieving a $\alpha_{Ce/La}$ = 3, though lower selectivity was observed for Nd(III)/Pr(III) separation. Tilp et al. [32] conducted the extraction of La(III) and Ce(III), also reporting a selectivity of $\alpha_{Ce/La}$ = 3. Olea et al. [33] utilized various β-diketones dissolved in hydrophobic ILs for the selective SX of an aqueous mixture of Ce and La, obtaining a selectivity of $\alpha_{Ce/La}$ = 1.74. In addition, deep eutectic solvents (DESs) have been explored for the extraction of REEs from mineral ores and electronic waste (e-waste) [34–37]. However, these systems have also demonstrated low selectivity [38]. This complex scenario highlights the pressing need for innovative strategies to improve selectivity in REE separation processes.

Membrane contactors represent an innovative approach to separation processes, offering improved efficiency and selectivity compared to traditional SX [39]. These devices utilize a porous membrane as a physical barrier between two liquid phases, enabling selective solute transfer based on differences in affinities and mass transfer rates. This

configuration simplifies operation, even when working with solvents of similar densities, while effectively minimizing issues such as flooding or solvent loss due to evaporation.

Membrane contactors enable the implementation of non-dispersive solvent extraction (NDSX), where an organic phase flowing through one side of the membrane wets the micropores, while a non-wetting aqueous phase passes along the other side. The aqueous-organic (aqueous–membrane) interface is effectively immobilized at the pore openings of the hydrophobic membrane support, through which solute mass transfer occurs. In particular, hollow fiber (HF)-based NDSX significantly overcomes the stability limitations observed in hollow fiber-supported liquid membranes (HF-SLMs) [40]. NDSX using membrane contactors has been successfully applied to the separation of REEs. For instance, Patil et al. [41] extracted Nd(III) from an aqueous medium into an organic phase using a commercial Liqui-Cel® HF module (3M Company, Charlotte, NC, USA), achieving quantitative extraction (>99%) within 30 min from a solution containing 1 g/L Nd(III) in 3.5 M HNO_3. However, selectivity between Nd(III) and Pr(III) remained low. Ambare et al. [40] explored an alternative organic phase and similarly achieved >99.9% recovery of Nd(III) within 30 min. Vernekar et al. [42] compared the performance of NDSX and an SLM using the same Liqui-Cel® module. Their results showed that NDSX exhibited faster extraction rates in the presence of H^+ ions, whereas the SLM was preferable in their absence. Several studies have demonstrated the excellent performance of the Liqui-Cel® module in REE separation processes [43,44].

Despite these promising results, neither the selectivity for adjacent REE separations nor the use of ILs as the receiving phase in NDSX with a commercial HF Liqui-Cel® module has been thoroughly evaluated. Given that the porous membrane introduces an additional resistance to mass transfer, the selective separation of Ce(III) over La(III) could potentially be enhanced compared to traditional SX. Moreover, using ILs as the receiving phase offers a high affinity for REEs, which can significantly improve their extraction efficiency. However, the viscosity of ILs introduces another resistance to mass transfer. This dual effect creates a separation system that not only provides a green and sustainable environment with a high affinity for REEs but may also achieve improved selectivity for Ce(III)/La(III) separation.

The objective of this study is to evaluate the selectivity in the separation of Ce(III) and La(III) ions from a synthetic aqueous sample using NDSX with an HF membrane contactor. Two extraction systems will be employed: Cyanex® 272 diluted in kerosene (industrial baseline) and the β-diketone 1,1,1-trifluoro-2,4-pentanedione (HTFAC) dissolved in the ionic liquid (IL) 1-octyl-3-methylimidazolium bis(trifluoromethylsulfonyl)imide ([Omim][Tf2n]). The latter was selected for its high hydrophobicity (0.18 mole fraction in water at 298.15 K) [45] and capacity to achieve high extraction percentages and selectivity values for REE separation [46]. HTFAC is employed because its strong complexation with REEs ensures effective transfer of the metal complex to the IL phase and Cyanex 272 is used because is a commercial extractant normally used for REE extraction [47–50]. This work aims to combine the extraction efficiency of the selected IL with the selectivity provided by the membrane and to assess how the additional mass transfer resistance influences the separation factor $\alpha_{Ce/La}$.

2. Experimental

2.1. Materials

Lanthanum(III) nitrate hexahydrate (99.999%), cerium(III) nitrate hexahydrate (99.99%), and the extractants 1,1,1-trifluoro-2,4-pentanedione (HTFAC) (98%) and tributyl phosphate (TBP, 97%) (ρ = 0.971 g/cm^3; μ = 3.399 mPa·s [51]) were purchased from Sigma-Aldrich® (Madrid, Spain). The diluent, Shellsol D-70® (ρ = 0.746 g/cm^3; μ = 1.070 mPa·s [52]), was supplied by Kremer GmbH (Aichstetten, Germany). The IL,

1-octyl-3-methylimidazolium bis(trifluoro- methylsulfonyl)imide ([Omim][Tf2n]) (>98%) (ρ = 1.32 g/cm^3; μ = 88.7 mPa·s [53]), was purchased from Iolitec GmbH (Heilbronn, Germany). Cyanex® 272 (ρ = 0.915 g/cm^3; μ = 120.000 mPa·s [54]) was purchased from Cytec Chile Ltda (Santiago, Chile). All reagents were used without further purification. Table 1 summarizes the reagents used in this work, including their molecular structures.

Table 1. Names and molecular structures of the extractants and diluents used in this study.

Chemical	Abbreviation	Function	Structure
Bis(2,4,4-trimethylpentyl)phosphinic acid	Cyanex® 272	Extractant	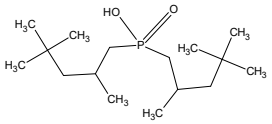
1,1,1-trifluoro-2,4-pentanedione	HTFAC	Extractant	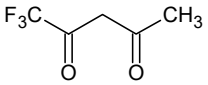
Tributyl phosphate	TBP	Synergistic agent	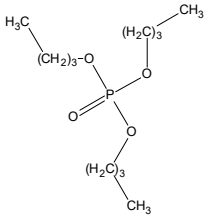
1-octyl-3-methylimidazolium bis((trifluoromethyl)sulfonyl)imide	[Omim][Tf2n]	Diluent	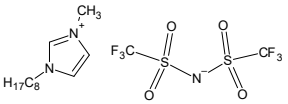

2.2. Solvent Extraction Procedure

Prior to the NDSX experiments, SX experiments were performed to determine extraction efficiency and selectivity at equilibrium. Aqueous solutions of La(III) and Ce(III) (1.44 mM) were prepared by dissolving the respective salts in ultrapure water (18.2 MΩ·cm, purified with a Milli-Q device, Millipore® (Madrid, Spain)). The initial pH was adjusted with 0.1 M H_2SO_4, and both the initial and equilibrium pH were measured using a pH meter Basic 20 (Crison®, Barcelona, Spain). The pH range of 3.7 to 5.2 studied in SX was chosen to cover the range from the pH at which the target metal ion starts to effectively interact with the extractant to the point where extraction efficiency begins to plateau.

The extracting phase consisted of Cyanex® 272 diluted in Shellsol D-70®, which was chosen for its high separation efficiency between adjacent light lanthanides [55]. Tributyl phosphate (TBP) was added to enhance the extraction [56], while 1,1,1-trifluoro-2,4-pentanedione (HTFAC) combined with the ionic liquid [Omim][Tf2n] was used to improve selectivity towards light lanthanides [33]. The selection of these extractants and the IL was based on the high purity of the reagents. The concentration chosen for the extractants was based on our previous work [33].

The SX experiments were conducted at 25 °C in an open flask, where 2 mL of the aqueous solution was mixed with 2 mL of the extracting phase and stirred for 2 h to ensure equilibrium was reached. Subsequently, the mixture was centrifuged for 40 min to facilitate phase separation. The aqueous phase was then carefully withdrawn from the vial, and the concentration of the remaining metal species in the aqueous phase was measured using inductively coupled plasma mass spectrometry (ICP-MS, model 7500 by Agilent® (l'Union, France)).

The efficiency of the solvent extraction process was evaluated by calculating the extraction percentage (%*E*), the distribution coefficient (*D*), and the selectivity (α_{ij}) defined by Equations (1)–(3):

$$\%E_i = \frac{D_i}{D_i + V_{aq}/V_{ext}} \quad (1)$$

$$D_i = \frac{C_{ext,i}}{C_{aq,i}} \quad (2)$$

$$\alpha_{ij} = \frac{D_i}{D_j} \quad (3)$$

where V_{ext} and V_{aq} represent the volumes of the extracting and aqueous phases, respectively. C_{ext} and C_{aq} are the concentrations of species "*i*" and "*j*" (in this research, Ce or La, respectively) in the extracting and aqueous phases at equilibrium, respectively.

2.3. Hollow Fiber Membrane Contactor

Figure 1 shows the schematic representation of the NDSX system. The metal solution (1.44 mM) containing La and Ce was pumped through the lumen of the fibers in the hollow contactor Liqui-Cel® (HF1 or HF2, specifications summarized in Table 2) supplied by Hoechst Celanese, using a Watson Marlow 323 peristaltic pump, in countercurrent flow with the extracting solution entering the shell side. A flow rate of 12.30 mL/min was used for the aqueous phase and 0.43 mL/min for the extracting phase to maintain a pressure difference of 0.1 bar in both phases, preventing the extraction phase from being dragged into the aqueous phase. The initial pH of the aqueous phase was adjusted to values between 2.0 and 5.0, while the temperature of both phases was maintained at 25 °C.

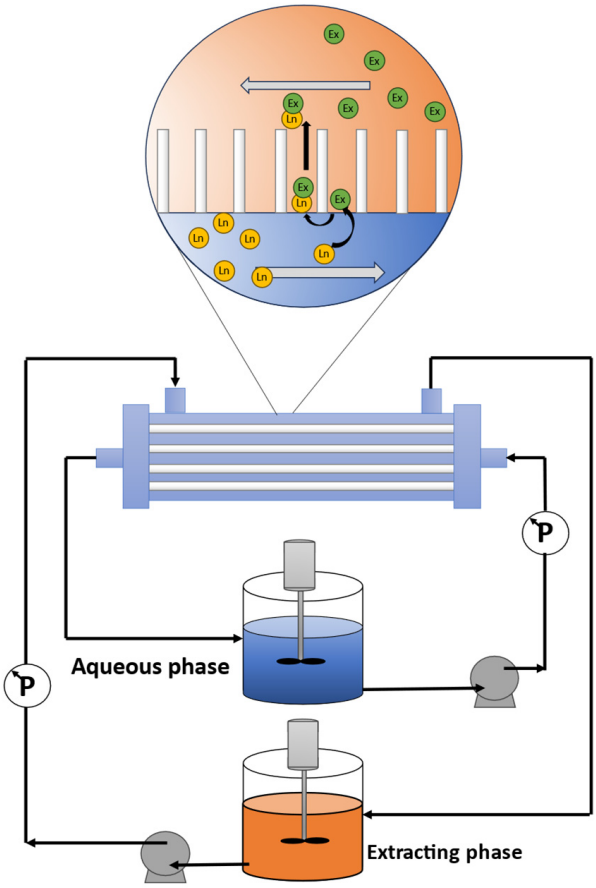

Figure 1. Schematic diagram of NDSX system of lanthanides with a hollow fiber membrane.

Table 2. Characteristics of the hollow fiber module used.

Characteristics	Value/Material	
	HF1	**HF2**
Fiber type	x-10/polypropylene	x-30/polypropylene
Internal diameter	240 µm	240 µm
Wall thickness	30 µm	30 µm
Number of fibers	2100	10,200
Nominal porosity	30%	40%
Shell material	Polypropylene	Polyethylene
Shell inner diameter	25 mm	54 mm
Shell length	200 mm	255 mm
Effective mass-transfer length	160 mm	146 mm
Effective mass-transfer area	0.23 m^2	1.4 m^2

3. Results and Discussion

3.1. NDSX with Cyanex® 272 Diluted in Shellsol D-70 Using HF1

Figure 2 shows the SX experiments performed to determine the optimal initial pH for introducing the aqueous phase into the HF contactor. The results indicate that the lowest extraction efficiencies (%E) are observed when the initial pH is 5.6, with extraction percentages slightly increasing as the initial pH is reduced. Cyanex® 272 is a weak organic acid with a pKa value of 6.37 [57], meaning that at an initial pH of 5.6, a significant portion of the extractant is protonated, rendering it ineffective for extraction. Other studies have also reported a slight increase in La(III) and Ce(III) extraction when using Cyanex® 272 at lower initial pH values [49,55]. Additionally, the $\alpha_{Ce/La}$ increases as the equilibrium pH rises, as demonstrated by Kashi et al. [55] in the separation of Nd(III) from La(III). The high concentration of H_2SO_4 likely favors the formation of monosulfate complexes, such as $LnSO_4^+$ [58,59], where hydrogen bonds may form between the sulfate oxygen and the protons from protonated Cyanex® 272. This, combined with the small concentration of deprotonated Cyanex® 272 in the pH range of 3.6–5.2, is sufficient to achieve extraction percentages of 40% for La(III) and 10% for Ce(III). Finally, for the NDSX system, an initial aqueous pH of 5.6 was selected as it provides the highest selectivity in the SX experiments.

After the equilibrium experiments, extractions in the HF module were conducted. Figure 3 presents the results from the NDSX process using HF1. It is observed that the selectivity for Ce increases over time, although it does not reach a constant value. In the NDSX system, both extraction efficiency and selectivity exceed those observed in the equilibrium SX experiments, which yielded $\%E_{La}$ = 3.1, $\%E_{Ce}$ = 27, and $\alpha_{Ce/La}$ = 12.7. This can be explained by the fact that, in these NDSX experiments, the equilibrium pH is not reached (pH_{eq} = 2.01 in SX), with a final pH of 2.08 after 120 min.

During the extraction using NDSX, the same lanthanide complex is formed as in the aqueous phase during the equilibrium SX experiments [33]. This complex then encounters the pore of the HF membrane, which is filled with the extracting solvent (kerosene + Cyanex® 272) and is subsequently transferred into the bulk of the extracting phase. Thus, the mass transfer process exhibits three main resistances: the aqueous phase, the membrane pore, and the extracting phase, with the major resistances being those associated with the membrane pore and the extracting phase [60]. According to Viega et al. [61], the resistance through the porous membrane is significantly influenced by the diffusion coefficient, which, in this case, refers to the diffusion of the complex in the membrane pore that is filled with the extracting phase. If the extraction conditions, membrane characteristics, and solvents are the same for both La(III) and Ce(III), the only difference can be attributed to the molar volume of the complex, which affects diffusion

through the porous membrane, as described by the Wilke–Chang or Scheibel equations, and the kinetic extraction reaction occurring at the aqueous/extracting phase interface in the membrane pore.

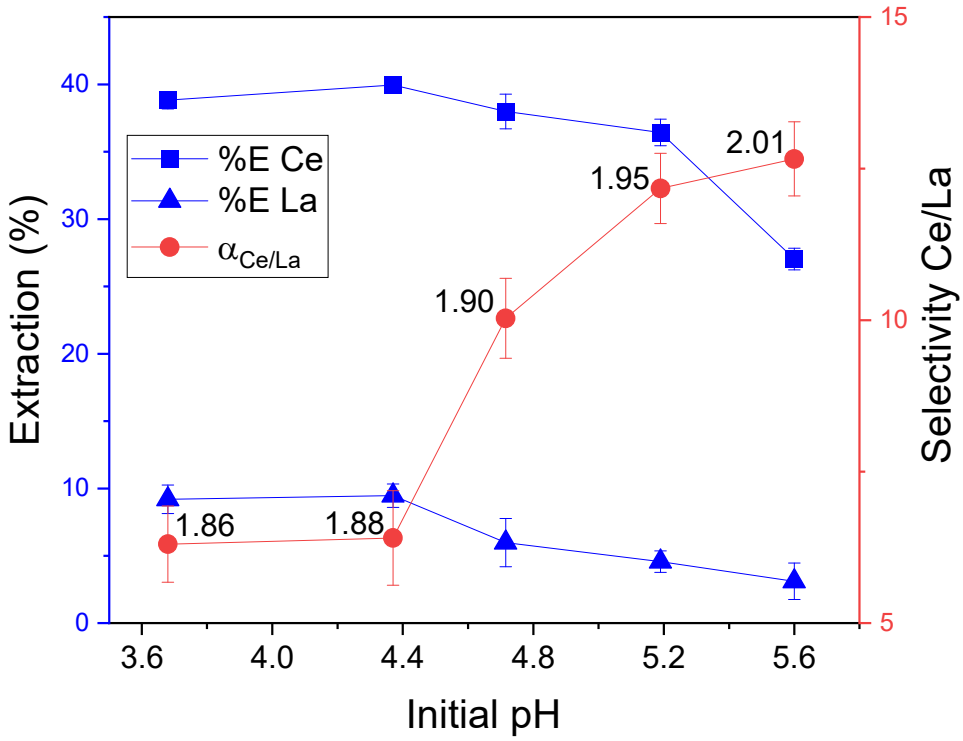

Figure 2. SX of La and Ce using 0.4 M Cyanex® 272 diluted in Shellsol D-70 at different initial pH values. Both phases were maintained at 25 °C. The aqueous metal concentration was set to $[La^{3+}] = [Ce^{3+}] = 1.44$ mM. The phase ratio (organic/aqueous) is 1:1. The values shown in the graph correspond to the equilibrium pH.

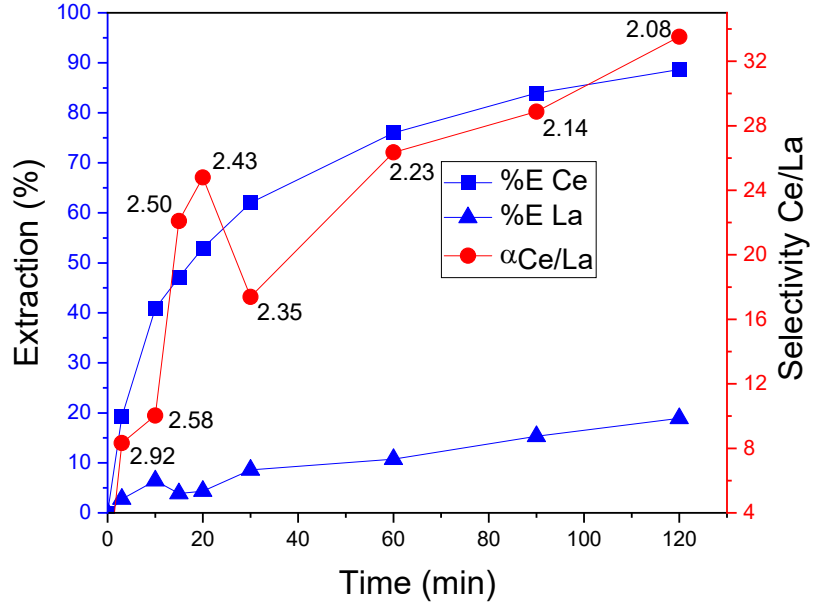

Figure 3. Extraction using HF1 with recirculation of both the aqueous and extracting phases. The feed solution has an initial pH of 5.6. The aqueous metal concentration was set to $[La^{3+}] = [Ce^{3+}] = 1.44$ mM. The receiving phase consists of 0.4 M Cyanex® 272 diluted in Shellsol D-70. The phase ratio (organic/aqueous) is 1:1. Both phases were maintained at 25 °C. The values shown in the graph correspond to the pH.

To study the effect of diffusion coefficients, it is essential to analyze the extraction mechanism of light lanthanides in equilibrium. Previous studies have experimentally determined that three moles of Cyanex® 272 form a complex with the lanthanide at a $pH_{eq} \approx 3$ [62]. The phosphinic group in Cyanex® 272 should be structurally oriented toward the lanthanide cation, and since the same hydration number can be considered between Ce and La [63], the Ln-O bond length will dominate the molar volume of the complex. According to Xue et al. [64], the Ln-O bond length is shorter for Ce(III) than for La(III) due to lanthanide contraction. Based on the Hard Soft Acid Base (HSAB) theory, Ce(III) is expected to behave as a harder acid than La(III) (i.e., more capable of accepting electrons) due to the additional proton. This results in a higher density charge on the metal and, consequently, a smaller molar volume. To further investigate diffusion, molecular geometry optimizations were performed using DFT calculations with the def-TZVP basis set and BP86-D3 functional [65]. The Ln complexes obtained are shown in Figure 4, and the resulting molar volumes are presented in Table 3. From this, a lower molar volume for Ce complexes was found, suggesting a higher diffusion rate for Ce(III).

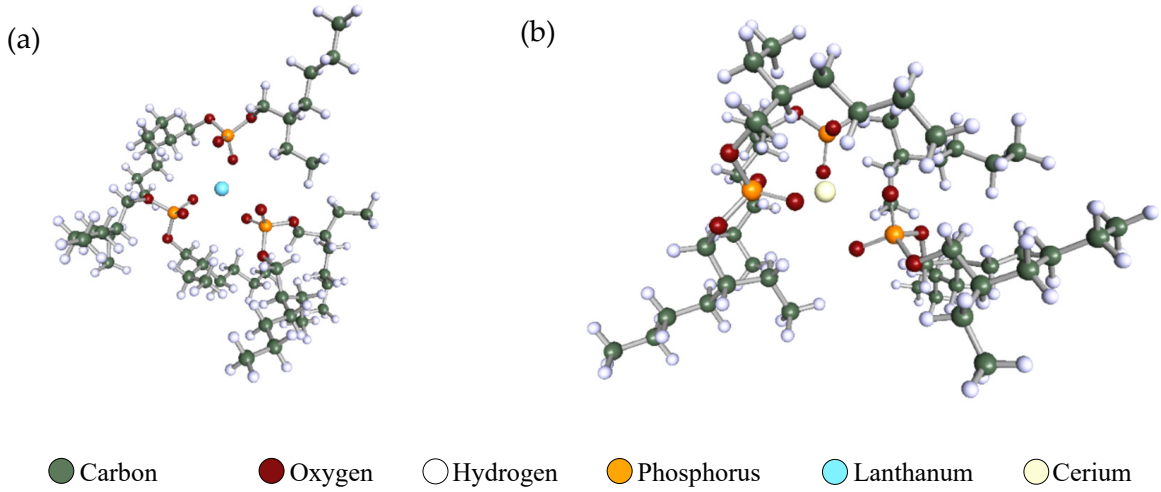

Figure 4. Molecular structures optimized using Turbomole® (version 4.4.1) for the determination of the complex volumes. (**a**) La(Cyanex® 272)$_3$ and (**b**) Ce(Cyanex® 272)$_3$.

Table 3. Molar volumes of La and Ce complexes with Cyanex® 272 optimized using Turbomole (def-TZVP basis set and BP86-D3 functional).

Complex	Molar Volume (Å^3)
La(Cyanex272)$_3$	1320.7
Ce(Cyanex272)$_3$	1298.8

The preferential extraction of Ce(III) over La(III) can be explained by the smaller ionic radius of Ce, which increases its kinetic complexation with Cyanex® 272, due to the decrease in activation energy [66]. The smaller complex volume also accounts for the lower mass transfer resistance offered by the membrane pore for Ce. Additionally, the distribution constant at a given pH is higher for the Ce-Cyanex® 272 complex in organic diluent [65,67]. The chemical potential is closely related to a concentration gradient, which drives mass transfer. In this context, the concentration gradient is the difference between the concentration in the aqueous phase and the maximum solubility in the extractant phase. As the comparative solubility increases—such as between Ce and La—Ce will exhibit a higher mass gradient than La, leading to enhanced transfer. All this leads to a higher selectivity for Ce compared to a simple equilibrium SX.

Another observation is that after 3 min, a rapid decrease in pH occurs due to the deprotonation of Cyanex® 272 near the aqueous/extracting phase boundary layer. Subsequently, a more gradual pH drop is observed as the system reaches equilibrium. This could be explained by the presence of extractants at the interface at the beginning, where $3H^+$ ions must be exchanged for each metal ion extracted to maintain a charge balance between the two phases. Once the extractants have interacted with the metal, the pH drop becomes more gradual, as the extractant must diffuse through the membrane pores from the bulk extracting phase to the interface. The release of protons from the extractant is kinetically more favorable than the metal complexation. This controlled release promotes the extraction of Ce, as discussed above.

To increase the extraction rates and selectivity towards Ce, it was proposed to maintain the optimal initial pH conditions, as shown in Figure 5. For this purpose, the aqueous phase was maintained at pH 5.0 by adding aliquots of 0.1 M NaOH solution to the aqueous stream. Additionally, a pH of 2.2 was maintained to simulate more realistic conditions in an SX plant operating under more acidic conditions. After 20 min, with a constant pH of 2.2 (Figure 5a), extractions close to 60% were obtained, due to the low availability of the acid extractant. Meanwhile, when the pH was maintained at 5.0 (Figure 5b), Ce extraction approached 100%, even higher than in the system without pH control. This is because the deprotonation of the extractant is promoted at these pH values (pKa Cyanex® 272 = 6.37 [57]). It is important to note that the values of these constants will depend, as expected, on how they were measured, the composition of the aqueous phase (ionic strength and anion present), and the nature of the diluent in the extracting phase [67]. Therefore, different pKa values for Cyanex® 272 can be found in the literature [68–70]. Although extractions increased in the latter case, the selectivity values were lower than in the run without pH control ($\alpha_{Ce/La}$ = 33). However, by maintaining an optimal pH of 5.0 for the deprotonation of the acid extractant, a precipitate formed due to the saponification of Cyanex® 272 with NaOH, and the experimental runs were stopped after 25 min. These results highlight the clear advantages of using NDSX over SX for selectively separating REE elements. The non-equilibrium operation, with the additional mass transfer resistance, leads to better selectivity, as does the control of the pH in the aqueous phase, which is not as easy to achieve in SX.

Figure 5b illustrates how, despite the increasing extraction of both metals, the selectivity continues to rise, even when the concentrations appear to equalize graphically. This behavior is due to the definition of selectivity based on the distribution constants (as defined by Equation (3)). This method is widely adopted in the literature because it provides a standardized framework for comparing results across different studies and experimental setups. Additionally, since the metals were measured by ICP-MS, high sensitivity in the concentration measurements can be achieved. This results in the distribution constant of cerium increasing significantly at the final experimental time point, when the extraction is nearly 100%. However, the use of concentration ratios in the organic phase as an alternative metric for selectivity is both valid and insightful. For instance, as demonstrated by the data in Figure 5a, the concentration ratio is significantly higher than the ratio observed in Figure 5b. This metric provides a straightforward and practical way to assess selectivity, particularly when considering the final composition of the organic phase for downstream processes. It can also be more intuitive for evaluating the feasibility of separation under specific conditions. Nevertheless, the use of distribution coefficients remains advantageous for theoretical and comparative purposes. By normalizing the selectivity calculation to the equilibrium concentrations in the aqueous and organic phases, the distribution coefficient approach inherently accounts for variations in phase volumes, initial concentrations, and system-specific factors, ensuring consistency and reproducibility.

(a)

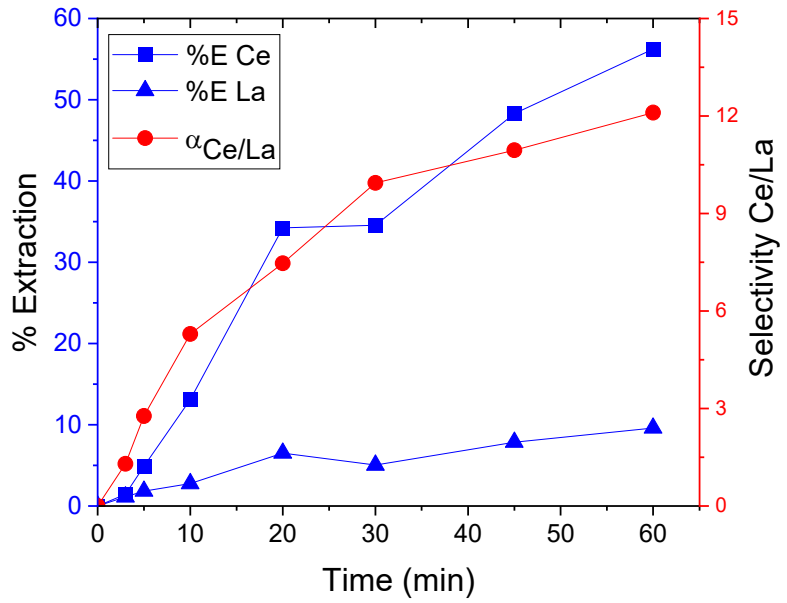

(b)

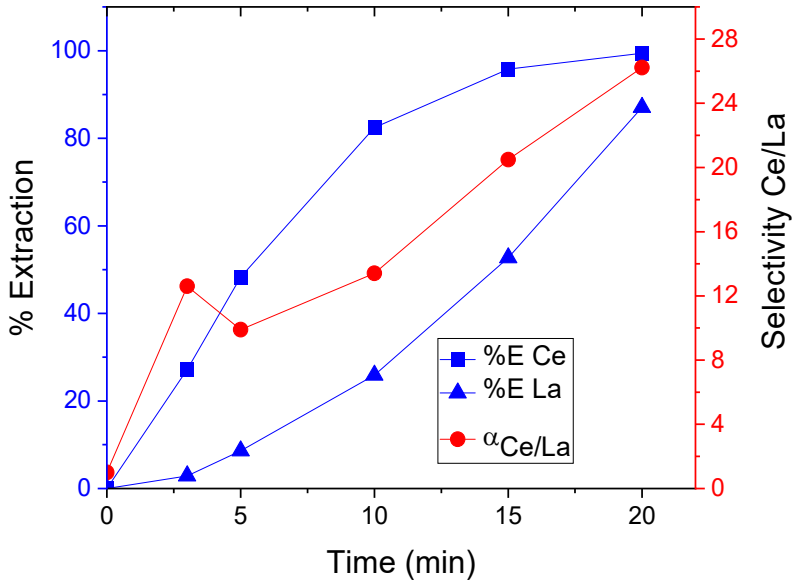

Figure 5. Extraction using the membrane contactor with recirculation of the aqueous and extracting phase. Feed solution maintained at (**a**) pH = 2.2 and (**b**) pH = 5.0 with NaOH 0.1 M. Receiving phase Cyanex® 272 0.4 M diluted in Shellsol D-70. The aqueous metal concentration was set to $[La^{3+}] = [Ce^{3+}] = 1.44$ mM. Both phases were maintained at 25 °C. Phase ratio extracting/aqueous 1:1.

3.2. NDSX with HTFAC and TBP Diluted in [Omim][Tf2n] Using HF1

When HTFAC extractant is used in conjunction with ILs, two main advantages over the system with kerosene can be identified: (1) ILs have a higher viscosity than kerosene, and this additional mass transfer resistance for the transfer of the complex to the IL solvent could enhance selectivity, as discussed previously and (2) ILs provide a greener alternative for the extraction of metal ions [71]. Figure 6 presents the experimental results from NDSX membrane extractions using HTFAC as the extractant, TBP as the phase modifier, and [Omim][Tf2n] as the diluent when the pH in the aqueous phase is maintained at 3.5 and 5.6 with 0.1 M NaOH. Compared to the previous system using Cyanex® 272 diluted in

Shellsol D-70, lower extraction efficiencies are observed. This can be attributed to the high viscosity of the IL, which limits mass transfer both during the deprotonation of HTFAC (pKa = 6.09 [72]) and the transfer of the complex to the IL phase. As shown in Figure 6a, despite lower Ce extractions, high selectivity is achieved after 20 min. The mass transfer limitation results in negligible La extraction until approximately 30 min. Furthermore, this process operates at an acidic pH of 3.5, which could enable moderate extraction and selectivity under conditions closer to those found in industrial PLS, thus eliminating the need to basify the aqueous phase.

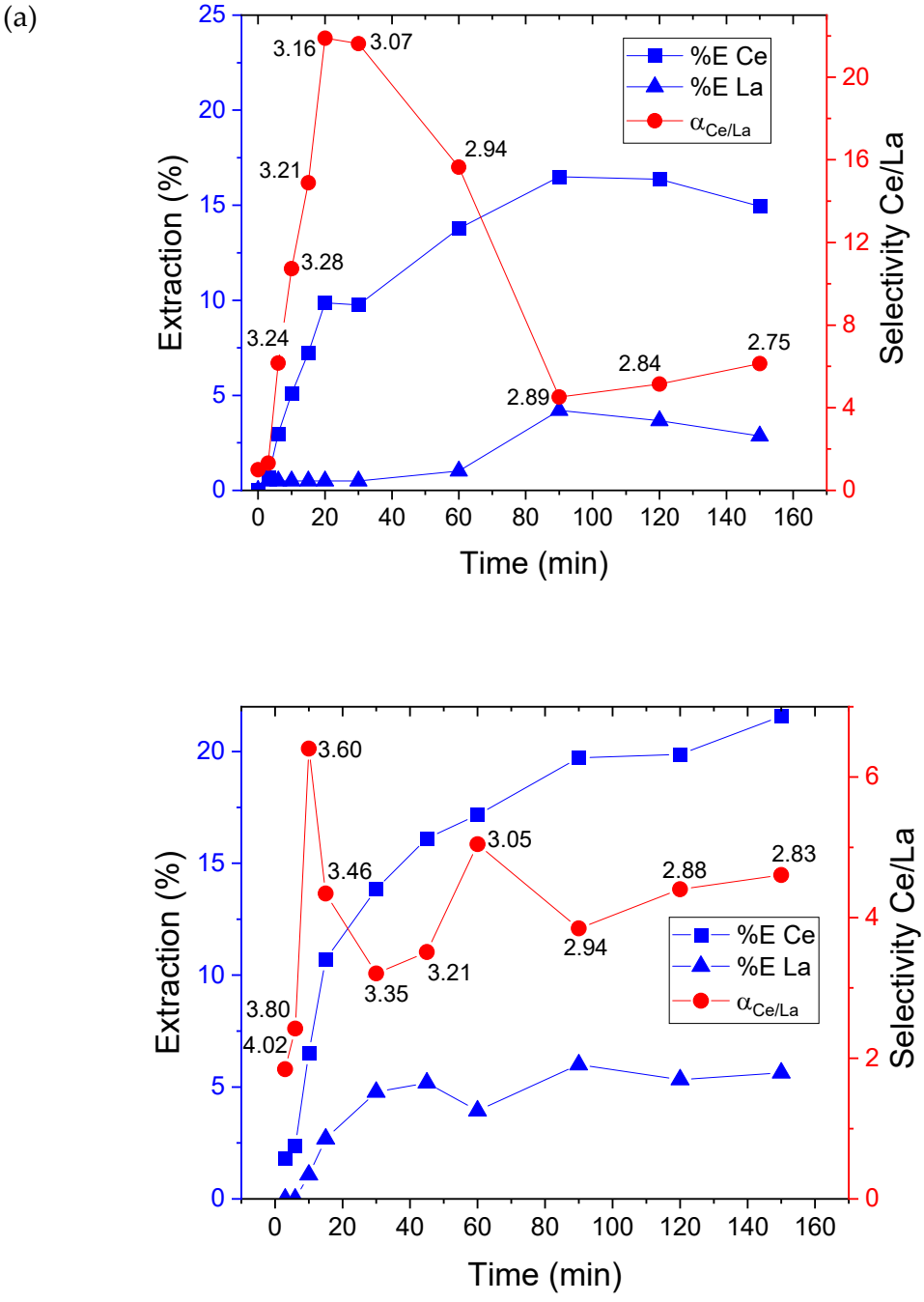

Figure 6. Extraction using the membrane contactor with recirculation of the aqueous and extracting phases, maintaining a feed solution at pH = 3.5 (**a**) and pH = 5.6 (**b**) with NaOH 0.1 M. The aqueous metal concentration was set to $[La^{3+}] = [Ce^{3+}] = 1.44$ mM. The receiving phase consists of HTFAC 0.4 M and TBP 0.04 M diluted in [Omim][Tf2n]. The phase ratio (extracting/aqueous) is 1:1. Both phases were maintained at 25 °C. The values indicated in the graph correspond to the pH.

As can be seen in Figure 6b, at a constant pH of 5.6, slightly higher extraction efficiencies are observed for both metals, due to the increased availability of HTFAC extractant. However, since La(III) is extracted from the beginning, selectivity is lower compared to the experiments performed at lower pH values. On the other hand, in both experiments conducted at a constant pH in the aqueous phase, the highest selectivity is achieved around 15–20 min. This time frame is much shorter compared to the system with kerosene, which can be attributed to the additional mass transfer resistance posed by the IL (the viscosity of [Omim][Tf2n] and Shellsol D-70 at 298.15 K is 88.7 mPa·s [53] and ~1.07 mPa·s [52], respectively). After this period, selectivity begins to decline due to a slight increase in the extraction percentages of La(III). This mass transfer limitation provided by ILs offers promising potential for the selective separation of lanthanides. Finally, after 90 min, a decrease in the extractions of La(III) and Ce(III) is observed, indicating that chemical equilibrium is being reached in both phases.

It is important to note that comparisons between the two systems, Cyanex® 272 in kerosene and HTFAC in [Omim][Tf2n], may not be entirely suitable due to the different extraction percentages observed at equilibrium. However, since NDSX is primarily governed by mass transfer, the higher viscosity of the IL compared to kerosene still allows for the observation of selectivity changes, despite the differences in extraction efficiencies.

3.3. Extraction with HTFAC and TBP Diluted in [Omim][Tf2n] Using HF2

According to Table 2, when comparing the two HF modules, there is no difference in pore size, but rather in the surface area for mass transfer. HF2 exhibits a surface area six times larger than HF1, which allows for a higher metal extraction. This difference is illustrated in Figure 7, where Ce(III) extractions of 45% are achieved at a constant pH of 3.5, compared to only 15% with HF1. The high surface area provided by the HF2 membrane makes the process more similar to an SX process, offering faster extraction and, consequently, resulting in lower selectivity values for Ce(III). This issue could be addressed by increasing the flow rate of the aqueous phase, thereby reducing the residence time and promoting the extraction of Ce(III). Furthermore, Ce(III) extraction begins to decrease over time as the equilibrium pH is reached. Another factor could be that Ce(III) is changing its extraction mechanism. Initially, Ce(III) is extracted by the HTFAC extractants, forming $Ce(TFAC)_3$, but as time progresses, this complex may start interacting with the IL cations, forming the complex observed in SX, such as $(Ln(TFAC)_4[Omim])$ [33,73,74]. This would typically result in higher extraction of La(III) at equilibrium, but due to the non-equilibrium nature of the system, Ce(III) extraction is initially favored.

Some challenges may arise when using ILs as an extractant phase in an NDSX system. Due to their higher viscosity, ILs can increase the associated costs of agitation and transport to the membranes. Additionally, their viscosity limits transmembrane fluxes, needing larger contact areas. To address these issues, the next step is to design an IL phase with slightly lower viscosity and better affinity for the formed complex, resulting in higher extraction efficiency and improved selectivity. On the other hand, polypropylene membranes offer a high melting point, as well as chemical and mechanical stability [75–77]. However, they may suffer from fouling or sweating, which can decrease the flux. To address this, various solutions are available, such as coating the surface to increase hydrophobicity or functionalizing the surface, among others [78,79].

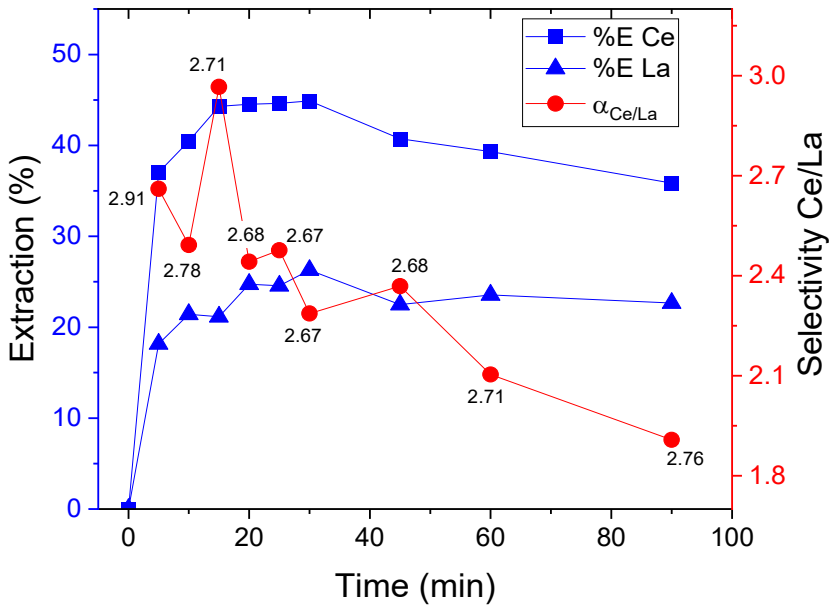

Figure 7. Extraction using HF2 with recirculation of the aqueous and extracting phases, maintaining a feed solution at pH = 3.5 with NaOH 0.1 M. The aqueous metal concentration was set to $[La^{3+}] = [Ce^{3+}] = 1.44$ mM. Receiving phase: HTFAC 0.4 M and TBP 0.04 M diluted in [Omim][Tf2n]. Phase ratio extracting/aqueous = 1:1. Both phases were maintained at 25 °C. The values indicated in the graph correspond to the pH.

Finally, HF membranes could provide high selectivity in REE extraction, which is a challenge when using SX, especially for separating adjacent REEs [46]. The HF membrane offers extra resistance to mass transfer, enabling selective separation. However, to enhance the practical relevance of this study, it is essential to expand its scope to evaluate the method's performance in real-world scenarios, such as the separation of REEs from mining operations, industrial waste, or electronic scrap. Industrial waste and electronic scrap are rich sources of REEs but have significant challenges due to the complex matrices in which these elements are found. These materials often contain impurities and a wide range of other metals, which can interfere with the selective extraction processes. Key performance indicators to consider include the extraction efficiency, selectivity, and stability of the extracting phase under realistic conditions over time. Pre-treatment steps might be required to concentrate the REEs or to remove bulk impurities. The membrane contactor's ability to handle such pre-treated feeds, while maintaining high separation efficiency and reducing cross-contamination, could provide critical insights into its practical viability.

4. Conclusions

This study demonstrates the potential of hollow fiber (HF) membrane contactors for the selective separation of La(III) and Ce(III) using non-dispersive solvent extraction (NDSX). Initially, equilibrium SX experiments using Cyanex® 272 as the extractant and kerosene as the diluent showed that the pH of the aqueous solution providing the highest selectivity was 5.6. In contrast, NDSX experiments exhibited even higher selectivity ($\alpha_{Ce/La} = 34$) after 120 min of operation. However, when the pH of the aqueous solution is maintained constant using a NaOH solution in the NDSX system, a selectivity of $\alpha_{Ce/La} = 26$ can be obtained after 20 min of operation. When the extracting phase is composed of the extractant HTFAC and TBP diluted in IL [Omim][Tf2n], a slight decrease in selectivity ($\alpha_{Ce/La} = 22$) is observed after 20 min, offering moderate extraction efficiencies and shorter times for achieving peak selectivity. An increase in the surface area for mass transfer in the membrane (HF2 experiments) results in a higher extraction rate

but significantly decreases selectivity due to its approximation to an SX stage. Finally, in this work, promising results for the selective separation of adjacent REEs were shown, which opens the possibility for HF membranes to be used industrially in the recovery of these valuable elements from different sources. However, several challenges remain: it is necessary to conduct experiments using a real PLS containing multiple REEs, as well as to perform immediate stripping to regenerate the extractant phase and determine the optimal operating conditions.

Author Contributions: Conceptualization, F.O. and L.U.; Methodology, L.U. and J.R.; Software, L.U.; Formal analysis, F.O. and R.A.; Resources, E.B.; Data curation, F.O.; Writing—original draft, F.O. and E.Q.-M.; Writing—review & editing, F.O., J.U.-A., R.A., J.R. and E.Q.-M.; Visualization, J.U.-A.; Supervision, E.B.; Project administration, E.Q.-M.; Funding acquisition, E.B. and E.Q.-M. All authors have read and agreed to the published version of the manuscript.

Funding: This research was funded by the Project Fondecyt 1211234 from the National Agency for Research and Development (ANID) and Dicyt 051911QM_PAP from the University of Santiago de Chile. Felipe Olea thanks the National Agency for Research and Development (ANID)/Scholarship Program/DOCTORADO NACIONAL/2019—21191785.

Data Availability Statement: The data are included within the article.

Conflicts of Interest: The authors declare no conflicts of interest related to this study.

References

1. Yan, D.; Ro, S.; Sunam, O.; Kim, S. On the Global Rare Earth Elements Utilization and Its Supply-Demand in the Future. *IOP Conf. Ser. Earth Environ. Sci.* **2020**, *508*, 012084. [CrossRef]
2. Cheng, S.; Li, W.; Han, Y.; Sun, Y.; Gao, P.; Zhang, X. Recent Process Developments in Beneficiation and Metallurgy of Rare Earths: A Review. *J. Rare Earths* **2024**, *42*, 629–642. [CrossRef]
3. Esmaeili-Zare, M.; Amiri, O. Rare Earth-Based Compounds for Solar Cells. In *Advanced Rare Earth-Based Ceramic Nanomaterials*; Zinatloo-Ajabshir, S., Ed.; Elsevier: Amsterdam, The Netherlands, 2022; pp. 365–393. ISBN 978-0-323-89957-4. [CrossRef]
4. Heim, J.W.; Vander Wal, R.L. NdFeB Permanent Magnet Uses, Projected Growth Rates and Nd Plus Dy Demands across End-Use Sectors through 2050: A Review. *Minerals* **2023**, *13*, 1274. [CrossRef]
5. Lin, B.; Zhang, Y.; Li, W.; Huang, J.; Yang, Y.; Or, S.W.; Xing, Z.; Guo, S. Recent Advances in Rare Earth Compounds for Lithium–Sulfur Batteries. *eScience* **2024**, *4*, 100180. [CrossRef]
6. Hossain, M.K.; Ahmed, M.H.; Khan, M.I.; Miah, M.S.; Hossain, S. Recent Progress of Rare Earth Oxides for Sensor, Detector, and Electronic Device Applications: A Review. *ACS Appl. Electron. Mater.* **2021**, *3*, 4255–4283. [CrossRef]
7. Tripathi, H.S.; Karmakar, R.; Bhowmik, T.K.; Halder, S.; Dutta, A.; Sinha, T.P. $RCoO_3$ {R = Pr, Nd and Sm} Electrode-Based for Efficient Solid-State Symmetric Supercapacitor. *Solid State Sci.* **2022**, *134*, 107065. [CrossRef]
8. Shen, Y.; Jia, Y.; Chen, F. Femtosecond Laser-Induced Optical Waveguides in Crystalline Garnets: Fabrication and Application. *Opt. Laser Technol.* **2023**, *164*, 109528. [CrossRef]
9. Ramalho, J.F.C.B.; Carneiro Neto, A.N.; Carlos, L.D.; André, P.S.; Ferreira, R.A.S. Lanthanides for the New Generation of Optical Sensing and Internet of Things. In *Including Actinides*; Bünzli, J.-C.G., Pecharsky, V.K., Eds.; Elsevier: Amsterdam, The Netherlands, 2022; Volume 61, pp. 31–128, ISSN 0168-1273, ISBN 9780323985949. [CrossRef]
10. Lucchetti, L.E.B.; Autreto, P.A.S.; Santos, M.C.; de Almeida, J.M. Cerium Doped Graphene-Based Materials towards Oxygen Reduction Reaction Catalysis. *Mater. Today Commun.* **2024**, *38*, 108461. [CrossRef]
11. Shi, Y.; Liu, T.; Wang, Z.; Zhao, X.; Zeng, L. Cerium Dioxide Based Nanoprobe with Self-Accelerating Cascade Catalysis for Enhanced Catalytic Therapy by Self-Generating H_2O_2 and Reducing PH Value. *Chem. Eng. J.* **2023**, *474*, 145513. [CrossRef]
12. Xu, Y.; Zhou, Y.; Li, Y.; Liu, Y.; Ding, Z. Advances in Cerium Dioxide Nanomaterials: Synthesis Strategies, Property Modulation, and Multifunctional Applications. *J. Environ. Chem. Eng.* **2024**, *12*, 113719. [CrossRef]
13. Chen, T.-B.; Rabiee, H.; Yan, P.; Zhu, Z.; Ge, L. Enhancing the Ammonia Catalytic Decomposition of Lanthanum Strontium Titanate Nickel Perovskite Catalysts via a Balanced Cation Doping and Deficiency Strategy. *Energy Fuels* **2024**, *38*, 5449–5456. [CrossRef]
14. Afiqah-Idrus, A.; Abdulkareem-Alsultan, G.; Asikin-Mijan, N.; Fawzi Nassar, M.; Voon, L.; Hwa Teo, S.; Agustiono Kurniawan, T.; Athirah Adzahar, N.; Surahim, M.; Zulaika Razali, S.; et al. Deoxygenation of Waste Sludge Palm Oil into Hydrocarbon Rich Fuel over Carbon-Supported Bimetallic Tungsten-Lanthanum Catalyst. *Energy Convers. Manag. X* **2024**, *23*, 100589. [CrossRef]

15. Wu, Z.; Li, X.; Jiang, P.; Feng, G.; Cao, L.; Wang, X.-M.; Tan, R.; Feng, E. Mechanical Milling Promotes the Preparation of Catalyst Lanthanum Dodecyl Sulfate and Green Solvent-Free Grinding for Synthesis of N-Heterocyclic Derivatives. *Appl. Catal. A Gen.* **2024**, *684*, 119893. [CrossRef]
16. Guo, N.; Wang, Z.; Yuan, C.; Wang, Z.; Jiang, L.; Wang, Q.; Du, Z.; Liu, Y. Insights into Catalytic Oxidation Mechanism of Toluene by Lanthanum Mangan-Based Perovskite in Wet Environment Based on in-Situ DRIFTS. *Sep. Purif. Technol.* **2025**, *353*, 128296. [CrossRef]
17. Alharshan, G.A.; Elamy, M.I.; Ebrahem, N.M.; Mahmoud, A.M.A.; Rammah, Y.S.; Elsad, R.A.; Misbah, M.H.; Said, S.A. Physical, Structural, and Optical Characteristics of the Glasses System Based on Lanthanum-Doped Phosphate. *Opt. Quantum Electron.* **2024**, *56*, 1179. [CrossRef]
18. Topper, B.; Neumann, A.; Mafi, A.; Pettes, M.; Alrubkhi, A.; Wilke, S.K.; Weber, R. Nonlinear Optical Properties of Lanthanum Titanate Glasses Prepared by Levitation Melting. *Appl. Phys. Lett.* **2024**, *124*, 94104. [CrossRef]
19. Ilyas, S.; Ranjan Srivastava, R.; Kim, H. Solvent Extraction for High Separation Strategy of Light and Heavy Rare Earth Elements from a Sulfate-Leached Solution of Low-Grade Monazite. *Sep. Purif. Technol.* **2024**, *341*, 126896. [CrossRef]
20. Zhang, K.; Wei, B.; Tao, J.; Zhong, X.; Zhu, W.; Wang, R.; Liu, Z. Recovery of Rare Earth Elements from Deep-Sea Mud Using Acid Leaching Followed by Selective Solvent Extraction with N1923 and TBP. *Sep. Purif. Technol.* **2023**, *318*, 124013. [CrossRef]
21. Dewulf, B.; Riaño, S.; Binnemans, K. Separation of Heavy Rare-Earth Elements by Non-Aqueous Solvent Extraction: Flowsheet Development and Mixer-Settler Tests. *Sep. Purif. Technol.* **2022**, *290*, 120882. [CrossRef]
22. Dzulqornain, A.M.; Cueva-Sola, A.B.; Chung, K.W.; Lee, J.-Y.; Jyothi, R.K. Strategy for Possible Separation of Light Rare Earth Elements (La, Ce, Pr, Nd) from Synthetic Chloride Solutions by Oxidative Precipitation, Solvent Extraction and Stripping. *Hydrometallurgy* **2024**, *224*, 106242. [CrossRef]
23. Belfqueh, S.; Chapron, S.; Giusti, F.; Pellet-Rostaing, S.; Seron, A.; Menad, N.; Arrachart, G. Selective Recovery of Rare Earth Elements from Acetic Leachate of NdFeB Magnet by Solvent Extraction. *Sep. Purif. Technol.* **2024**, *339*, 126701. [CrossRef]
24. Zhang, W.; Feng, D.; Xie, X.; Tong, X.; Du, Y.; Cao, Y. Solvent Extraction and Separation of Light Rare Earths from Chloride Media Using HDEHP-P350 System. *J. Rare Earths* **2022**, *40*, 328–337. [CrossRef]
25. Tunsu, C.; Ekberg, C.; Foreman, M.; Retegan, T. Studies on the Solvent Extraction of Rare Earth Metals from Fluorescent Lamp Waste Using Cyanex 923. *Solvent Extr. Ion Exch.* **2014**, *32*, 650–668. [CrossRef]
26. Sharma, C.R.; Patadia, R.N.; Agrawal, Y.K. Solvent Extraction, Sequential Separation and Trace Determination of La (III), Ce (III), Nd (III) and Gd (III) with 2, 14-Bis[m-Nitrophenyl]-Calix[4]Resorcinarene-8, 20-Bis[N-Phenylbenzo]-Dihydroxamic Acid. *Solvent Extr. Ion Exch.* **2023**, *41*, 606–626. [CrossRef]
27. Arrachart, G.; Couturier, J.; Dourdain, S.; Levard, C.; Pellet-Rostaing, S. Recovery of Rare Earth Elements (REEs) Using Ionic Solvents. *Processes* **2021**, *9*, 1202. [CrossRef]
28. Wang, K.; Adidharma, H.; Radosz, M.; Wan, P.; Xu, X.; Russell, C.K.; Tian, H.; Fan, M.; Yu, J. Recovery of Rare Earth Elements with Ionic Liquids. *Green Chem.* **2017**, *19*, 4469–4493. [CrossRef]
29. Kim, B.K.; Lee, E.J.; Kang, Y.; Lee, J.J. Application of Ionic Liquids for Metal Dissolution and Extraction. *J. Ind. Eng. Chem.* **2018**, *61*, 388–397. [CrossRef]
30. Yudaev, P.A.; Chistyakov, E.M. Ionic Liquids as Components of Systems for Metal Extraction. *ChemEngineering* **2022**, *6*, 6. [CrossRef]
31. Quinn, J.E.; Soldenhoff, K.H.; Stevens, G.W. Solvent Extraction of Rare Earth Elements Using a Bifunctional Ionic Liquid. Part 2: Separation of Rare Earth Elements. *Hydrometallurgy* **2017**, *169*, 621–628. [CrossRef]
32. Tilp, A.H.; Akl, H.M.; Kandil, A.E.H.T.; Cheira, M.F.; Gado, H.S.; Salah, B.A. Extraction of La, Ce, and Nd Using an Ionic Liquid and Its Application to Rare Earth Leachate Derived from Phosphogypsum. *J. Rare Earths* 2024, *in press*. [CrossRef]
33. Olea, F.; Rosales, G.; Quintriqueo, A.; Romero, J.; Pizarro, J.; Ortiz, C.; Quijada-Maldonado, E. Theoretical Prediction of Selectivity in Solvent Extraction of La(III) and Ce(III) from Aqueous Solutions Using β-Diketones as Extractants and Kerosene and Two Imidazolium-Based Ionic Liquids as Diluents via Quantum Chemistry and COSMO-RS Calculations. *J. Mol. Liq.* **2021**, *325*, 114655. [CrossRef]
34. Karan, R.; Sreenivas, T.; Kumar, M.A.; Singh, D.K. Recovery of Rare Earth Elements from Coal Flyash Using Deep Eutectic Solvents as Leachants and Precipitating as Oxalate or Fluoride. *Hydrometallurgy* **2022**, *214*, 105952. [CrossRef]
35. Feng, F.; Wang, M.; Zhang, J.; Ding, H.; Yu, L.; Guo, W.; Guo, L.; Liang, Q.; Zhang, Q.; Lu, C.; et al. Hydrogen Bonding-Based Deep Eutectic Solvents for Choline Chloride/Sulfamide and Its Application in the Recycling of Precious Metals. *J. Environ. Chem. Eng.* **2024**, *12*, 113611. [CrossRef]
36. Liu, Z.; Yang, F.; Sun, Z.; Chi, Q.; Li, Y. Efficient Selective Leaching of Ytterbium and Lutetium Oxides by New Hydrophobic Deep Eutectic Solvents. *Sep. Purif. Technol.* **2024**, *343*, 127097. [CrossRef]
37. Entezari-Zarandi, A.; Larachi, F. Selective Dissolution of Rare-Earth Element Carbonates in Deep Eutectic Solvents. *J. Rare Earths* **2019**, *37*, 528–533. [CrossRef]

38. Hanada, T.; Schaeffer, N.; Katoh, M.; Coutinho, J.A.P.; Goto, M. Improved Separation of Rare Earth Elements Using Hydrophobic Deep Eutectic Solvents: Liquid–Liquid Extraction to Selective Dissolution. *Green Chem.* **2024**, *26*, 9671–9675. [CrossRef]
39. Mansourizadeh, A.; Rezaei, I.; Lau, W.J.; Seah, M.Q.; Ismail, A.F. A Review on Recent Progress in Environmental Applications of Membrane Contactor Technology. *J. Environ. Chem. Eng.* **2022**, *10*, 107631. [CrossRef]
40. Ambare, D.N.N.; Ansari, S.A.A.; Anitha, M.; Kandwal, P.; Singh, D.K.K.; Singh, H.; Mohapatra, P.K.K. Non-Dispersive Solvent Extraction of Neodymium Using a Hollow Fiber Contactor: Mass Transfer and Modeling Studies. *J. Membr. Sci.* **2013**, *446*, 106–112. [CrossRef]
41. Patil, C.B.; Ansari, S.A.; Mohapatra, P.K.; Natarajan, V.; Manchanda, V.K. Non-Dispersive Solvent Extraction and Stripping of Neodymium (III) Using a Hollow Fiber Contactor with TODGA as the Extractant. *Sep. Sci. Technol.* **2011**, *46*, 765–773. [CrossRef]
42. Vernekar, P.V.; Jagdale, Y.D.; Patwardhan, A.W.; Patwardhan, A.V.; Ansari, S.A.; Mohapatra, P.K. Non-Dispersive Solvent Extraction of Neodymium Using N,N,N′,N′ -Tetraoctyl Diglycolamide (TODGA). *Sep. Sci. Technol.* **2014**, *49*, 1541–1554. [CrossRef]
43. Hernández-Pellón, A.; Gallart Tauler, L.E.; Ibañez, R.; Ortiz, I.; San-Román, M.-F. New Challenges and Applications of Supported Liquid Membrane Systems Based on Facilitated Transport in Liquid Phase Separations of Metallic Species. *J. Membr. Sci. Res.* **2022**, *8*. [CrossRef]
44. Yadav, K.K.; Singh, D.K.; Kain, V. Separation of Terbium from Aqueous Phase Employing Hollow Fibre Supported Liquid Membrane with EHEHPA as Carrier. *Sep. Sci. Technol.* **2019**, *54*, 1521–1532. [CrossRef]
45. Freire, M.G.; Carvalho, P.J.; Gardas, R.L.; Marrucho, I.M.; Santos, L.M.N.B.F.; Coutinho, J.A.P. Mutual Solubilities of Water and the [C n Mim][Tf 2 N] Hydrophobic Ionic Liquids. *J. Phys. Chem. B* **2008**, *112*, 1604–1610. [CrossRef] [PubMed]
46. Quijada-Maldonado, E.; Romero, J. Solvent Extraction of Rare-Earth Elements with Ionic Liquids: Toward a Selective and Sustainable Extraction of These Valuable Elements. *Curr. Opin. Green Sustain. Chem.* **2021**, *27*, 100428. [CrossRef]
47. Reddy, B.R.; Kumar, J.R. Rare Earths Extraction, Separation, and Recovery from Phosphoric Acid Media. *Solvent Extr. Ion Exch.* **2016**, *34*, 226–240. [CrossRef]
48. Xiong, Y.; Wu, D.; Li, D.; Meng, S. Kinetics of Y(III) Stripping for the System Y/HCl/Cyanex 272-P507/Heptane with Constant Interfacial Area Cell with Laminar Flow. *Solvent Extr. Ion Exch.* **2005**, *23*, 803–816. [CrossRef]
49. İnan, S.; Tel, H.; Sert, Ş.; Çetinkaya, B.; Sengül, S.; Özkan, B.; Altaş, Y. Extraction and Separation Studies of Rare Earth Elements Using Cyanex 272 Impregnated Amberlite XAD-7 Resin. *Hydrometallurgy* **2018**, *181*, 156–163. [CrossRef]
50. Mohammedi, H.; Miloudi, H.; Tayeb, A.; Bertagnolli, C.; Boos, A. Study on the Extraction of Lanthanides by a Mesoporous MCM-41 Silica Impregnated with Cyanex 272. *Sep. Purif. Technol.* **2019**, *209*, 359–367. [CrossRef]
51. Tian, Q.; Liu, H. Densities and Viscosities of Binary Mixtures of Tributyl Phosphate with Hexane and Dodecane from (298.15 to 328.15) K. *J. Chem. Eng. Data* **2007**, *52*, 892–897. [CrossRef]
52. Koekemoer, L.R.; Badenhorst, M.J.G.; Everson, R.C. Determination of Viscosity and Density of Di-(2-Ethylhexyl) Phosphoric Acid + Aliphatic Kerosene. *J. Chem. Eng. Data* **2005**, *50*, 587–590. [CrossRef]
53. Aljasmi, A.; AlJimaz, A.S.; Alkhaldi, K.H.A.E.A.E.; Altuwaim, M.S. Dependency of Physicochemical Properties of Imidazolium Bis(Trifluoromethylsulfonyl)Imide-Based Ionic Liquids on Temperature and Alkyl Chain. *J. Chem. Eng. Data* **2022**, *67*, 858–868. [CrossRef]
54. Biswas, R.K.; Singha, H.P. Densities, Viscosities and Excess Properties of Bis-2,4,4-Trimethylpentylphosphinic Acid (Cyanex 272) + Diluent Binary Mixtures at 298.15 K and Atmospheric Pressure. *J. Mol. Liq.* **2007**, *135*, 179–187. [CrossRef]
55. Kashi, E.; Habibpour, R.; Gorzin, H.; Maleki, A. Solvent Extraction and Separation of Light Rare Earth Elements (La, Pr and Nd) in the Presence of Lactic Acid as a Complexing Agent by Cyanex 272 in Kerosene and the Effect of Citric Acid, Acetic Acid and Titriplex III as Auxiliary Agents. *J. Rare Earths* **2018**, *36*, 317–323. [CrossRef]
56. Yudaev, P.A.; Kolpinskaya, N.A.; Chistyakov, E.M. Organophosphorous Extractants for Metals. *Hydrometallurgy* **2021**, *201*, 105558. [CrossRef]
57. Sole, K.C.; Hiskey, J.B. Solvent Extraction of Copper by Cyanex 272, Cyanex 302 and Cyanex 301. *Hydrometallurgy* **1995**, *37*, 129–147. [CrossRef]
58. Judge, W.D.; Ng, K.L.; Moldoveanu, G.A.; Kolliopoulos, G.; Papangelakis, V.G.; Azimi, G. Solubilities of Heavy Rare Earth Sulfates in Water (Gadolinium to Lutetium) and H_2SO_4 Solutions (Dysprosium). *Hydrometallurgy* **2023**, *218*, 106054. [CrossRef]
59. Moldoveanu, G.A.; Kolliopoulos, G.; Judge, W.D.; Ng, K.L.; Azimi, G.; Papangelakis, V.G. Solubilities of Individual Light Rare Earth Sulfates (Lanthanum to Europium) in Water and H_2SO_4 Solutions (Neodymium Sulfate). *Hydrometallurgy* **2024**, *223*, 106194. [CrossRef]
60. Juang, R.-S.; Huang, H.-L. Mechanistic Analysis of Solvent Extraction of Heavy Metals in Membrane Contactors. *J. Membr. Sci.* **2003**, *213*, 125–135. [CrossRef]
61. Viegas, R.M.; Rodríguez, M.; Luque, S.; Alvarez, J.; Coelhoso, I.; Crespo, J.P.S. Mass Transfer Correlations in Membrane Extraction: Analysis of Wilson-Plot Methodology. *J. Membr. Sci.* **1998**, *145*, 129–142. [CrossRef]
62. Park, H.J.; Tavlarides, L.L. Adsorption of Neodymium(III) from Aqueous Solutions Using a Phosphorus Functionalized Adsorbent. *Ind. Eng. Chem. Res.* **2010**, *49*, 12567–12575. [CrossRef]

63. Cotton, S.A. Establishing Coordination Numbers for the Lanthanides in Simple Complexes. *Comptes Rendus Chim.* **2005**, *8*, 129–145. [CrossRef]
64. Xue, D.; Zuo, S.; Ratajczak, H. Electronegativity and Structural Characteristics of Lanthanides. *Phys. B Condens. Matter* **2004**, *352*, 99–104. [CrossRef]
65. Olea, F.; Durán, G.; Díaz, G.; Villarroel, E.; Araya-López, C.; Cabezas, R.; Merlet, G.; Romero, J.; Quijada-Maldonado, E. Ionic Liquids for the Selective Solvent Extraction of Lithium from Aqueous Solutions: A Theoretical Selection Using COSMO-RS. *Minerals* **2022**, *12*, 190. [CrossRef]
66. Rogalski, M.H.; Dang, A.N.; Mezyk, S.P. Evaluation of the Arrhenius Behavior of N-Dodecane Radical Cation ($RH^{\cdot}$+) Reactivity with Lanthanide Ion-Complexed N,N,N′,N′-Tetraoctyl Diglycolamide (TODGA). *Phys. Chem. Chem. Phys.* **2024**, *27*, 1960–1967. [CrossRef] [PubMed]
67. Biswas, R.K.; Habib, M.A.; Singha, H.P. Colorimetric Estimation and Some Physicochemical Properties of Purified Cyanex 272. *Hydrometallurgy* **2005**, *76*, 97–104. [CrossRef]
68. Yilmaz, A.; Arslan, G.; Tor, A.; Akin, I. Selectively Facilitated Transport of Zn(II) through a Novel Polymer Inclusion Membrane Containing Cyanex 272 as a Carrier Reagent. *Desalination* **2011**, *277*, 301–307. [CrossRef]
69. Das, D.; Juvekar, V.A.; Rupawate, V.H.; Ramprasad, K.; Bhattacharya, R. Effect of the Nature of Organophosphorous Acid Moiety on Co-Extraction of U(VI) and Mineral Acid from Aqueous Solutions Using D2EHPA, PC88A and Cyanex 272. *Hydrometallurgy* **2015**, *152*, 129–138. [CrossRef]
70. Pakarinen, J.; Paatero, E. Effect of Temperature on Mn–Ca Selectivity with Organophosphorus Acid Extractants. *Hydrometallurgy* **2011**, *106*, 159–164. [CrossRef]
71. El-Shaheny, R.; El Hamd, M.A.; El-Enany, N.; Alshehri, S.; El-Maghrabey, M. Insights on the Utility of Ionic Liquids for Greener Recovery of Gold and Silver from Water, Wastes, and Ores. *J. Mol. Liq.* **2024**, *414*, 126034. [CrossRef]
72. Serine, T.; Inaba, K.; Morimoto, T. Distribution Equilibria of Five β-Diketones and Their Complexes of Copper (II) and Iron (III) in 4-Methyl-2-Pentanone- Aqueous Perchlorate Solution Systems. *Anal. Sci.* **1986**, *2*, 535–540. [CrossRef]
73. Jensen, M.P.; Borkowski, M.; Laszak, I.; Beitz, J.V.; Rickert, P.G.; Dietz, M.L. Anion Effects in the Extraction of Lanthanide 2-Thenoyltrifluoroacetone Complexes into an Ionic Liquid. *Sep. Sci. Technol.* **2012**, *47*, 233–243. [CrossRef]
74. Billard, I.; Ouadi, A.; Gaillard, C. Liquid–Liquid Extraction of Actinides, Lanthanides, and Fission Products by Use of Ionic Liquids: From Discovery to Understanding. *Anal. Bioanal. Chem.* **2011**, *400*, 1555–1566. [CrossRef]
75. Petukhov, D.I.; Komkova, M.A.; Eliseev, A.A.A.A.; Poyarkov, A.A.; Eliseev, A.A.A.A. Nanoporous Polypropylene Membrane Contactors for COH_2 and H_2S Capture Using Alkali Absorbents. *Chem. Eng. Res. Des.* **2022**, *177*, 448–460. [CrossRef]
76. Kim, K.; Lee, H.; Park, H.S.; Song, H.; Kim, S. Surface Modification of Polypropylene Hollow Fiber Membranes Using Fluorosilane for CO_2 Absorption in a Gas-Liquid Membrane Contactor. *Heliyon* **2023**, *9*, e19829. [CrossRef] [PubMed]
77. Amirabedi, P.; Akbari, A.; Yegani, R. Fabrication of Hydrophobic PP/CH_3SiO_2 Composite Hollow Fiber Membrane for Membrane Contactor Application. *Sep. Purif. Technol.* **2019**, *228*, 115689. [CrossRef]
78. Pabby, A.K.; Sastre, A.M. State-of-the-Art Review on Hollow Fibre Contactor Technology and Membrane-Based Extraction Processes. *J. Membr. Sci.* **2013**, *430*, 263–303. [CrossRef]
79. Yang, Y.F.; Wan, L.S.; Xu, Z.K. Surface Engineering of Microporous Polypropylene Membrane for Antifouling: A Mini-Review. *J. Adhes. Sci. Technol.* **2011**, *25*, 245–260. [CrossRef]